Antarct. Meteorite Res., **17**, 84–96, 2004

Origin of olivine megacrysts and the groundmass crystallization of the Dar al Gani 476 shergottite

Eisuke Koizumi*, Takashi Mikouchi, Akira Monkawa, and Masamichi Miyamoto

Department of Earth and Planetary Science, Graduate School of Science, University of Tokyo, Hongo, Bunkyo-ku, Tokyo 113-0033
**Corresponding author. E-mail: koi@eps.s.u-tokyo.ac.jp*

(Received March 11, 2004; Accepted June 17, 2004)

Abstract: The DaG 476 martian meteorite shows a porphyritic texture with megacrysts of olivine and orthopyroxene set in a groundmass of pyroxene and maskelynite. Previous studies on major and trace elements and isotopes of this meteorite implied a relationship to other martian meteorites. However, the origin of the olivine and orthopyroxene megacrysts is still under dispute, and therefore the formation of DaG 476 is unclear, although this sample is one of the most important martian meteorites. We performed crystallization experiments, a MELTS calculation and a cooling rate calculation to investigate the formation of DaG 476. The experimental and calculated results suggest that the parent melt of the DaG groundmass was more Fe- and Al-rich than the actual groundmass bulk composition, suggesting that the groundmass of DaG 476 contains a mafic cumulus component, alternatively fractionated liquid has escaped at the last crystallization stage. We evaluated three models for the origin of the olivine megacrysts (1) phenocryst origin, (2) xenocryst origin: homogeneous olivine was modified by exchange with the host magma and diffusion, and (3) xenocryst origin: chemical zoning of olivine was produced by the fractional crystallization. The mineralogy of DaG 476 and calculation results showed that all models were theoretically possible. However, models (1) and (2) need complex processes to produce observed natures of DaG 476. Hence, model (3) seems the most plausible, although this model also leaves some open questions. The fragment-like texture of olivine and the results of cooling rate calculation suggest that the formation of the DaG shergottites occurred in a rapid cooling condition in any of the formation models (1–3). Therefore, DaG seems to have crystallized near the martian surface.

key words: shergottite, olivine, pyroxene, chemical zoning, atomic diffusion

1. Introduction

Recently, several shergottites have been found from the desert areas of northern Africa and Middle East Asia (Meyer, 2003). Most of these new shergottites contain large olivine grains, although they were not present in "classic" basaltic shergottites such as Shergotty and Zagami (*e.g.*, McSween, 1994), and called olivine-phyric shergottite (*e.g.*, Goodrich, 2002, 2003). Olivine grains in these newly recovered shergottites are

mostly Mg-rich, but they show different mineralogical features in each meteorite. Dar al Gani 476 (DaG 476) and its paired samples (DaG 489/735/670/876/975) consist of olivine and orthopyroxene megacrysts set in a fine-grained groundmass of pyroxene and plagioclase (now shock-transformed into "maskelynite") with minor amounts of accessory minerals (spinel, merrillite, ilmenite and etc.) (*e.g.*, Mikouchi *et al.*, 2001) (Fig. 1). Olivine megacrysts are up to 5 mm in size, and are remarkably zoned from Fo_{76} in the core to Fo_{58} in the rim (Zipfel *et al.*, 2000; Folco *et al.*, 2000; Mikouchi *et al.*, 2001; Wadhwa *et al.*, 2001). Olivine shows variable shapes from nearly euhedral grains to anhedral grains, and some olivine grains look like fragments of larger grains. Orthopyroxene megacrysts reach ~0.3 mm in size, and show minor zoning, whose average composition is $En_{79}Fs_{19}Wo_2$ (Wadhwa *et al.*, 2001) although we could not find orthopyroxene megacryst in our thin section. Pyroxene in the groundmass is also extensively zoned ($En_{76}Fs_{21}Wo_3$~$En_{58}Fs_{30}Wo_{12}$) and more Mg-rich than those in the other basaltic and olivine-phyric shergottites. It has been pointed out that the pyroxene compositions of DaG 476 are more similar to those of lherzolitic shergottites ($En_{76}Fs_{21}Wo_3$~$En_{63}Fs_{22}Wo_{15}$) than to those of previously known basaltic shergottites (Mikouchi *et al.*, 2001). It is also reported that DaG 476 and its paired meteorites show petrological and mineralogical similarities to lithology A of EETA79001, which shows a porphyritic texture composed of olivine/orthopyroxene megacrysts set in a basaltic groundmass (*e.g.*, McSween and Jarosewich, 1983; Zipfel *et al.*, 2000). Major and trace element studies of olivine in lithology A of EETA 79001 and the lherzolitic shergottites also indicate similarities (*e.g.*, McSween and Jarosewich, 1983). Therefore, DaG shergottites, lithology A of EETA 79001 and lherzolitic shergottites show petrological similarities to each other, but they show distinct mineralogical and geochemical differ-

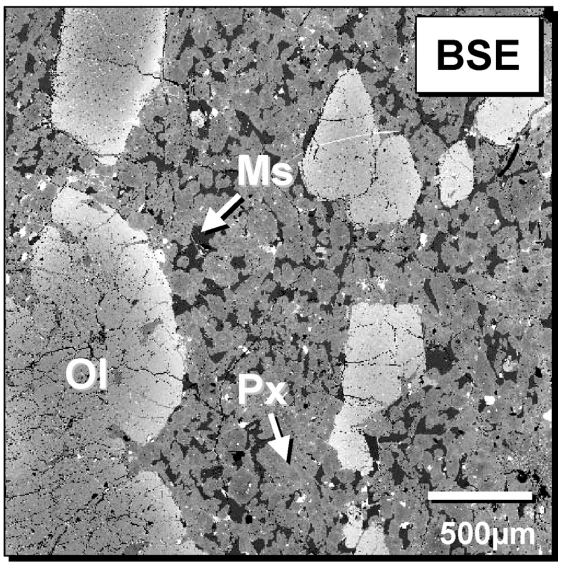

Fig. 1. Backscattered electron (BSE) image of DaG 476. Ol: olivine, Px: pyroxene, Ms: maskelynite.

ences from each other. In fact, isotopic and trace element studies suggested a closer genetic relationship between DaG 476 and Queen Alexandra Range (QUE) 94201, the nakhlites and Chassigny (Wadhwa *et al*., 2001). Thus, the discovery of the DaG shergottites is important in understanding the petrogenetic relationships among martian meteorites.

When we consider the crystallization history of DaG 476, olivine is a key mineral because there are two possible origins, either a phenocryst or xenocryst. Zipfel *et al*. (2000) indicated that textural irregularities between olivine megacryst and the groundmass shown in lithology A of EETA79001 were not observed in DaG 476, and they also pointed out that DaG olivines are present as single grains, although those in EETA79001 are xenoliths. According to these observations and other petrological features of DaG 476, they concluded that olivine and orthopyroxene megacrysts occurred as early phenocrysts. Borg *et al*. (2000) also preferred the phenocryst origin for olivine megacrysts because Sm-Nd isotopic data for olivine megacrysts fall on the isochron defined by maskelynite and pyroxene, suggesting that the olivine was in isotopic equilibrium with maskelynite and pyroxene. However, Wadhwa *et al*. (2001) reported that the estimated REE pattern of the melt in equilibrium with the orthopyroxene megacryst rim is LREE-enriched and is not parallel to that of the whole rock and the melts in equilibrium with the groundmass minerals, indicating that the orthopyroxene megacryst did not crystallize from the same parent melt of DaG groundmass minerals in a closed system although terrestrial weathering could cause LREE enrichment. Thus, they supported a xenocrystic origin for megacrysts in DaG shergottites. Some authors also suggested that olivine megacrysts derived from lherzolitic rocks as xenocrysts because of their mafic composition (*e.g*., Folco *et al*., 2000). However, recent work on another olivine-phyric shergottite SaU 005, which is similar to DaG 476 in the textural and compositional feature, by Goodrich (2003) concluded that the fraction of xenocrystic material is small although the most magnesian olivine and pyroxene are xenocrysts, and SaU 005 and lithology A of EETA 79001 did not form by mixing of basaltic shergottite-like melt and lherzolitic shergottite-like melt but from the parent melt of basaltic shergottites.

In this paper, we report the results of crystallization experiments using the bulk composition of DaG 476 to understand the crystallization sequence of this meteorite. At the same time, we calculated the phase assemblages of the DaG 476 groundmass composition using the MELTS program. By combining these results, we reevaluate the possible hypotheses for the origin of olivine megacrysts by utilizing the chemical zoning in these crystals.

2. Experimental procedures

We performed crystallization experiments using a compositional analog of DaG shergottites. All crystallization experiments were performed at Department of Earth and Planetary Science, University of Tokyo. We employed a combined experimental procedure used in Jurewicz *et al*. (1993), McKay *et al*. (1994), and Miyamoto and Mikouchi (1996). Synthetic glass having the average composition of the bulk compositions of DaG 476 and DaG 489 were prepared as the starting material (Table 1-a).

Table 1. The compositions of (a) DaG bulk, (b) starting glass of this study, (c) DaG groundmass bulk from this study and (4) DaG groundmass bulk from Zipfel et al. (2000).

	(a) DaG bulk (Average of Zipfel *et al.*, 2000 and Folco *et al.*, 2000)	(b) Starting glass	(c) DaG 476 groundmass (This study)	(d) DaG 476 groundmass (Zipfel *et al.*, 2000)
SiO_2	48.3	49.1	52.7	51.0
TiO_2	0.38	0.83	0.33	0.51
Al_2O_3	4.43	5.30	6.64	5.66
FeO	16.8	15.3	13.2	15.5
MnO	0.44	0.48	0.44	0.47
MgO	20.1	20.1	17.9	18.3
CaO	8.01	8.06	7.21	7.04
Na_2O	0.55	0.09	0.77	0.67
K_2O	0.04	0.04	-	-
Cr_2O_3	0.53	0.50	0.81	0.92
P_2O_5	0.42	0.14	-	-
Total	100	100	100	100

We added extra Fe to the starting material because Pt absorbs Fe during experiments (*e.g.*, McKay *et al.*, 1994). The obtained composition after homogenization is similar to the target composition (Table 1-b). Two pellets were made by pressing ~125 mg of the powdered starting material, and placing the pellets onto the Pt wire loops whose diameters are approximately 5 mm. Afterwards, they were suspended inside an alumina tube at the hot spot of a vertical 1 atm gas-mixing furnace for 48 hours to be homogenized at 1450°C, and quenched to room temperature. Then, they were put back into the furnace at the target temperature to crystallize minerals for 48 hours and quenched to room temperature again. Experimental temperatures were measured with thermocouples calibrated against the melting point of gold (1064.4°C). The precision of temperature control is within ±1°C (Miyamoto and Mikouchi, 1996). Oxygen fugacity was controlled at the estimated oxygen fugacity of DaG shergottites ($\log fO_2 =$ QFM−2.3, Herd *et al.*, 2002) by the gas mixture of CO_2-H_2, and gas flow rates were monitored by mass flow meters. Because of high experimental temperature, we did not measure the oxygen fugacity by zirconia cell in this series of experiments. The chemical compositions of minerals in the charges were obtained by electron probe microanalysis (EPMA) with the JEOL 8600 Super Probe at Department of Earth and Planetary Science, University of Tokyo (accelerating voltage of 15 kV and beam current of 12 nA). We used well-characterized natural and synthetic minerals as the standards for electron microprobe analysis. Mineral compositions of DaG 476 and lithology A of EETA79001 were also analyzed in thin section in order to compare these with compositions of synthetic minerals produced in these experiments. Because the glass composition was relatively Fe-poor near Pt wire due to the Fe absorption by Pt wire during the run, we analyzed the minerals that were present in the area over 100 μm away from Pt wire to avoid its influence. The synthetic olivine and pyroxene produced in this series of experiments usually have thin quench rims ($<3\,\mu$m) (Fig. 2). The high experimental temperatures due to the Mg-rich bulk composition of our starting material produced

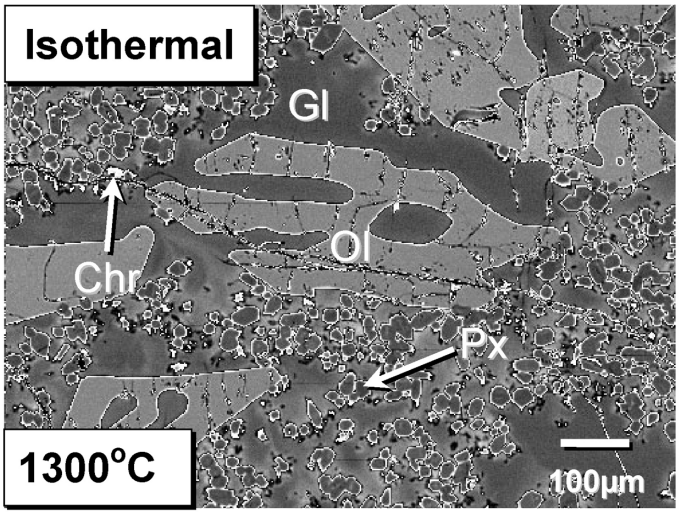

Fig. 2. BSE image of the run product from the isothermal experiment at 1300°C. Both olivine and pyroxene have the quench rims formed during the air quenching process. Ol: olivine, Px: pyroxene, Chr: chromite, Gl: glass.

the quench crystals during the air quenching. Hence, we analyzed cores of each minerals to avoid the influence of these quench rims.

3. Results and discussion

3.1. Crystallization experiment and the groundmass formation

The phase assemblages obtained from a series of the crystallization experiments are shown in Table 2, and Table 3 summarizes the chemical compositions of the phases present in the run charges. The 1425°C experiment contained only glass. Olivine was present in the experiment at 1400°C and lower temperatures. Therefore, the liquidus temperature of this composition is between 1425 and 1400°C. The size of the olivine grains is $\leq$~200 μm and their shapes are mostly euhedral. Many small orthopyroxene grains (~ a few tens of μm) and opaque mineral (chromite) ($<10\,\mu$m) were present in the 1300°C charge (Fig. 2). At this temperature olivine shows euhedral to skeletal shapes with subrounded corners and reach ~500 μm in size (Fig. 2). Olivines are homogeneous and their Fe contents increase as temperature becomes lower (from Fo_{88} at 1400°C to Fo_{85} at 1300°C). Olivine in the 1300°C experiment is still more Mg-rich than the olivine cores in DaG 476 (Fo_{76}) and lithology A of EETA79001 (Fo_{81}) (Fig. 3) (Mikouchi *et al*., 2001). These results agree with the MELTS calculation for a DaG 489 bulk composition as reported by Wadhwa *et al*. (2001). Thus, the olivines in our experiments are clearly more Mg-rich than that in DaG shergottites. This strongly suggests that the bulk composition of DaG shergottites does not represent their parent melt composition. The pyroxene that crystallized at 1300°C is probably orthopyroxene ($En_{83}Fs_{13}Wo_4$) (Fig. 3). The pyroxene is more Mg-rich than that in DaG 476 by about 8% of the enstatite component. The pyroxene composition of lithology A of EETA

Table 2. Phase assemblages of the isothermal experiments.

Temperature (°C)	Phase
1425	Glass
1400	Olivine (Fo_{88}), Glass
1375	Olivine (Fo_{87}), Glass
1350	Olivine (Fo_{87}), Glass
1300	Olivine (Fo_{86}), Pyroxene ($En_{83}Fs_{13}Wo_4$), Opaque, Glass

Table 3. Chemical composition of the phases from the isothermal experiments.

Temperature	1425	1400		1375		1350		1300			
Phase	Glass	Olivine	Glass	Olivine	Glass	Olivine	Glass	Olivine	Pyroxene	Opaque	Glass
SiO_2	49.08	40.18	50.22	39.95	52.43	40.41	53.67	40.54	57.00	0.12	49.26
TiO_2	5.30	0.02	0.87	0.04	1.14	0.02	1.12	0.01	0.15	1.11	1.55
Al_2O_3	0.38	0.03	4.54	0.04	5.97	0.03	6.04	0.03	0.55	7.28	7.32
FeO	15.3	11.78	14.47	12.46	15.34	12.49	13.51	13.57	8.82	18.97	13.85
MnO	0.48	0.34	0.51	0.37	0.53	0.37	0.50	0.45	0.42	0.53	0.36
MgO	20.08	48.06	20.41	46.58	12.42	46.86	13.30	46.63	31.45	11.66	13.47
CaO	8.06	0.25	8.22	0.24	10.74	0.27	10.36	0.32	2.28	0.23	13.15
Na_2O	0.09	-	0.02	-	0.03	-	0.02	-	0.00	-	0.01
K_2O	0.04	-	0.01	-	0.01	-	0.00	-	0.01	-	0.00
Cr_2O_3	0.53	0.24	0.47	0.25	0.54	0.27	0.47	0.22	0.54	60.37	0.25
P_2O_5	0.42	-	0.11	-	0.17	-	0.15	-	-	-	0.14
Total	99.97	100.90	99.84	99.93	99.32	100.72	99.13	101.79	101.78	100.26	99.39
Fo		12	-	13	-	13	-	14	-	-	
Fa		88	-	87	-	87	-	86	-	-	
En		-	-	-	-	-	-	-	83	-	
Fs		-	-	-	-	-	-	-	13	-	
Wo		-	-	-	-	-	-	-	4	-	

79001 is more Mg-rich ($En_{73}Fs_{22}Wo_5$) than that of DaG 476, but more Mg-poor than our synthetic pyroxene (Fig. 3) (although more magnesian pyroxene ($En_{81}Fs_{15}Wo_4$) of the possible xenocryst origin is reported in EETA79001 by McSween and Jarosewich (1983)). The Al contents of pyroxene in both DaG 476 and EETA79001 are clearly higher than that of our synthetic pyroxene (Fig. 4) although Ti and Cr contents do not show significant differences (Table 4).

We estimated the bulk composition of the DaG 476 groundmass by the grid analysis with the electron microprobe to investigate the formation of the groundmass of DaG shergottites. We defined groundmass as the area except olivine megacrysts (no orthopyroxene megacryst in our thin section). More than 1500 points of the groundmass were analyzed, and the average of these compositions is shown in Table 1-c. Silicon is higher and Fe and Mg are lower than in the bulk composition of DaG 476. However, the molar Fe/(Mg+Fe) ratio (fe#) of the bulk groundmass composition (fe#=0.29) is close to that of the bulk composition of whole DaG (fe#=0.32). The obtained composition is broadly similar to the estimated bulk groundmass composition by a mixing calculation (Table 1-d) (Zipfel *et al.*, 2000). We calculated a phase assemblage obtained from the bulk composition of the DaG groundmass (Table 1-c) by using the MELTS program (Ghiorso and Sack, 1995). The result shows that the liquidus phase of this composition is also olivine, whose composition (Fo_{88}) is equal to that of olivine that crystallized from the DaG bulk composition. These results indicate that the molar Fe/Mg ratio of the parent melt of the DaG groundmass is higher than

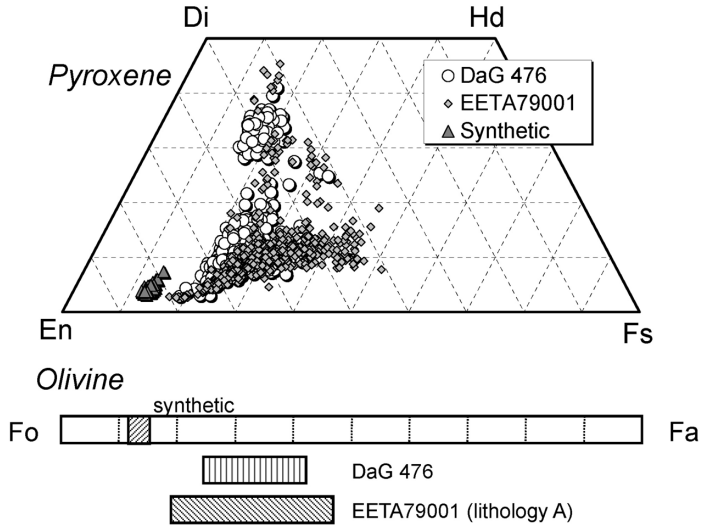

Fig. 3. Chemical compositions of synthetic olivine from the isothermal experiment at from 1400 to 1300℃, and synthetic pyroxene from the 1300℃ isothermal experiment along with those of DaG 476 and EETA79001 lithology A.

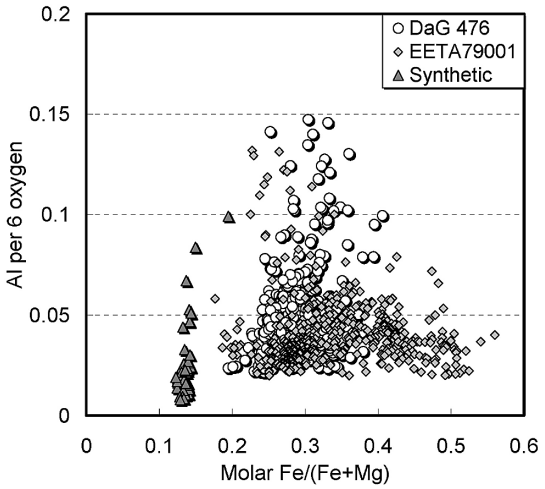

Fig. 4. Comparison of Al contents between the synthetic pyroxene from the 1300℃ isothermal experiment, DaG 476 and EETA79001 lithology A. Al was normalized against 6 oxygens.

Table 4. Comparison of the Al, Ti and Cr contents of pyroxenes in synthetic from this study, DaG 476 and lithology A of EETA79001.

	Synthetic	DaG 476	EETA79001 (lithology A)
Al_2O_3	0.19 - 0.80	0.58 – 1.36	0.38 – 1.31
TiO_2	0.05 – 0.54	0.05 – 0.81	0.03 – 0.89
Cr_2O_3	0.33 – 0.71	0.20 – 0.90	0.19 – 1.08

those of the bulk compositions of both whole DaG meteorite and the groundmass. One reason for this low Fe/Mg ratio of the bulk DaG groundmass composition is that the olivine megacrysts were dissolved and as a result the Mg contents of the melt, which already crystallized pyroxene cores, became higher when the olivine megacrysts were incorporated. However, the DaG olivine shows extensive Mg-Fe zoning and some of olivine grains show fragment-like textures, indicating that the DaG groundmass cooled fast enough to prevent re-equilibration of olivine with the groundmass melt. Hence, it is difficult that an assimilation of olivine megacrysts had been occurred. Considering the lower Al content of our synthetic pyroxenes than that of the groundmass pyroxene in DaG, it is plausible that the residual liquid poorer in Mg and richer in Al escaped, and the groundmass formed by a cumulus process. Thus, the parent melt of the groundmass should be more Fe- and Al-rich than its bulk composition.

3.2. Origin of olivine megacrysts

In this section, we discuss the origin of the olivine megacryst assemblage by investigating the following three models. Model (1) considers a phenocryst origin, and models (2) and (3) consider xenocryst origins.

(1) The first model assumes that olivine is a phenocryst and, hence, crystallized from the same melt as the parent melt of the groundmass pyroxene. Olivine started

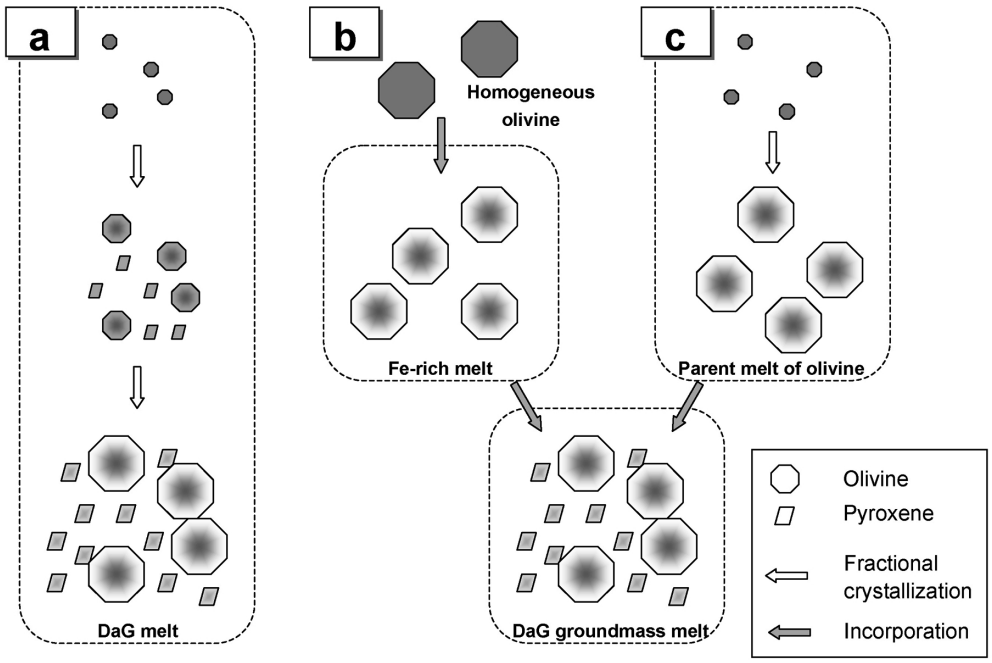

Fig. 5. Schematic illustration showing the hypothetical formation process of DaG 476. (a) Phenocryst origin model. (b) Xenocryst origin model: the atomic diffusion produced the chemical zoning of olivine from the homogeneous olivine. (c) Xenocryst origin model: fractional crystallization produced the chemical zoning of olivine.

crystallizing from the parent melt of DaG shergottites as a phenocryst, followed by pyroxene crystallization, and then both olivine and pyroxene grew producing chemical zoning by fractional crystallization (Fig. 5a). Then, accumulation of olivine and pyroxene occurred and plagioclase crystallized from the interstitial melt. We estimated the fe# of the parent melt that is in equilibrium with the cores of both olivine megacryst and groundmass pyroxene. The K_D(Fe/Mg) of 0.35 and 0.29 were adopted for exchange between olivine and melt, and pyroxene and melt, respectively. These exchange coefficients were obtained from the experimental results using the bulk composition of DaG (olivine) (this study) and QUE94201 (pyroxene) (Koizumi *et al*., 2001). The obtained fe#s are 0.41 for olivine (Fo_{76}) parent melt, and 0.49 for pyroxene ($En_{76}Fs_{21}Wo_3$) parent melt, suggesting that this model that olivine crystallized followed by the groundmass pyroxene crystallization, is reasonable if we consider that the parent melt becomes more Fe-rich after crystallization of olivine. However, some olivine grains in DaG shergottites have a fragment-like texture with the Mg-rich part that is located adjacent to the groundmass pyroxene and maskelynite (Figs. 1 and 6). This observation makes it very unlikely that the olivine megacrysts are phenocrysts.

(2) The second model assumes that the olivines are xenocrysts and that diffusion exchange with the liquid produced chemical zoning from originally homogeneous olivine.

We have modeled this process by matching the olivine zonation (Fig. 7). The diffusion calculation is similar to Miyamoto *et al*. (2002). Although some Mg-Fe

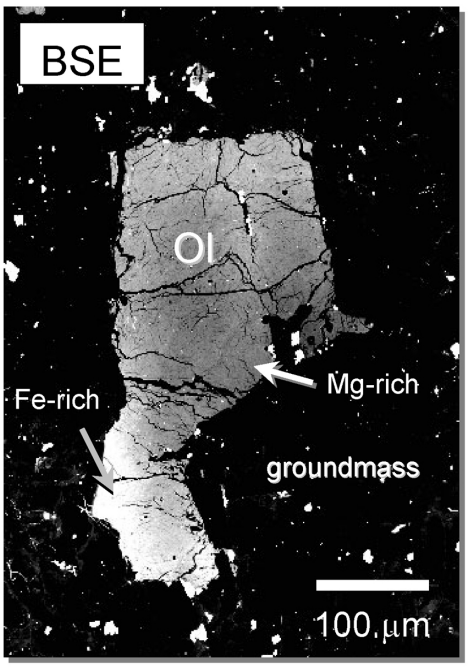

Fig. 6. BSE image of olivine megacryst in DaG 476 showing a fragment-like texture. Note the Mg-rich area is adjacent to the groundmass as Fe-rich area of olivine.

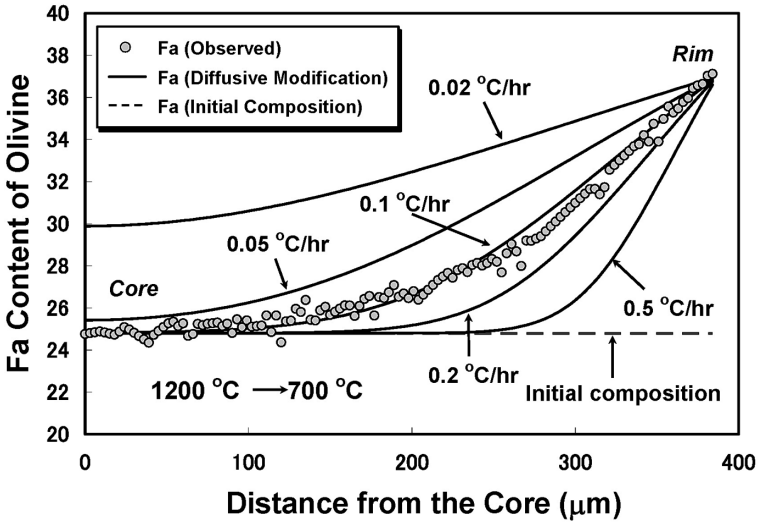

Fig. 7. Comparison of the result of diffusion calculations between the different cooling rates. The 0.1°C/hr cooling could reproduce the zoning profiles from the initial homogeneous olivine.

diffusion rates for olivine were reported by several different authors (*e.g.*, Buening and Buseck, 1973; Misener, 1974; Chakraborty, 1997), we adopted the diffusion coefficient reported by Misener (1974) because diffusion experiments by Miyamoto *et al*. (2002) gave the best fit between the observed diffusion profiles and those using the diffusion rate from Misener (1974). We calculated diffusion profiles for cooling over the temperature range of 1200–700°C because 1200°C is above the liquidus of the groundmass pyroxene by the calculation with the MELTS software, and it is possible to compare the results with those reported by Mikouchi *et al*. (2001). The calculation results show that atomic diffusion could reproduce the zoning pattern similar to that in DaG olivine, and the estimated cooling rate is about 0.1°C/hr (Fig. 7).

(3) The third model is that olivine crystallized from the comparatively Fe-rich melt by fractional crystallization producing chemical zoning, and was incorporated in the Mg-rich parent melt of the DaG groundmass (Fig. 5c) or the melt in which pyroxene in the groundmass has already started crystallizing. The cooling rate for olivine crystallization must have been rapid because fast cooling was necessary to keep the olivine zoned during the groundmass crystallization. Mikouchi *et al*. (2001) estimated a cooling rate of the DaG476 groundmass at 0.03–3°C/hr (0.4°C/hr is the same condition as that adopted for the model (2)) to prevent diffusive modification of the Mg-Fe zoning of olivine. This cooling rate also corresponds to the burial depth shallower than about 3 m at most.

Thus, model (3) is the only one that satisfactorily explains the observations of Fig. 6. However, the third model also leaves some open questions. In the parent melt of olivine megacrysts, pyroxene crystallization started immediately after the onset of olivine crystallization according to the estimated fe# of parent melts of both olivine and pyroxene (of course, other elemental contents slightly influence the liquidus tempera-

tures of olivine and pyroxene). Hence, it is inferred that abundant pyroxenes had been present in the parent melt of olivine megacrysts when olivine was incorporated into the parent melt of the DaG groundmass and, if so, there should be more abundant orthopyroxene megacrysts in DaG. Almost all megacrysts in DaG shergottites, however, are olivines. Thus, it is necessary to consider some geological process to remove olivine from pyroxene (*e.g.*, accumulation of either phase) in the parent melt of olivine megacryst before olivines were incorporated into the DaG groundmass. Furthermore, Mg-rich parts of fragment-like olivines have no influence of atomic diffusion, suggesting very rapid cooling of the DaG groundmass although the groundmass seems to be cumulate. Hence, some special condition is required to produce a "double" cumulate rock with rapid cooling history. In this model, it is difficult to consider that the olivine megacrysts derived from the same source of lherzolitic shergottites because no olivine that is zoned to as Fe-rich rim as that of DaG olivine is found so far.

Recently, Goodrich (2003) extensively studied magmatic inclusions in olivine, chromite and pyroxenes in SaU 005 and lithology A of EETA79001 and concluded that the most magnesian olivines in both meteorites are xenocrysts. Because the bulk chemistry and petrology of SaU 005 and DaG are almost identical, they clearly experienced the same formation history (*e.g.*, Goodrich, 2003). Thus, the xenocryst origin for the DaG olivine megacrysts suggested by this study is consistent with the result of Goodrich (2003) that the most magnesian olivine in SaU 005 is xenocryst. Goodrich (2003) also pointed out that the fraction of xenocrystic material is small (only a few percent) because SaU 005 and lithology A of EETA79001 must have lost fractionated melts late in their crystallization, which made the bulk compositions more magnesian. The REE data of the previous study (Wadhwa *et al.*, 2001) support the xenocryst origin hypothesis of olivine and orthopyroxene megacrysts in DaG, which is also consistent with the xenocryst model for the olivine megacrysts presented in this study.

4. Conclusions

The crystallization experiment of the bulk composition of DaG shergottites shows that olivine crystallized as a liquidus phase; however its composition is more Mg-rich than that of DaG shergottites. Also, synthetic pyroxenes are more Mg-rich and Al-poor than that of the DaG groundmass. These results suggest that the bulk composition of DaG does not represent its parent melt composition. Furthermore, the groundmass of the DaG shergottites also seems to include a mafic cumulus component because the calculation results with the MELTS software indicate that the liquidus phase of the bulk composition of the DaG groundmass is Mg-rich olivine (Fo_{88}) and the Al contents of synthetic pyroxene are lower than that in the DaG groundmass. The petrological observation and the result of the diffusion calculation of olivine megacrysts favor the model that the zoned olivines formed by fractional crystallization were incorporated into the parent melt of the DaG groundmass as xenocrysts. The results of our diffusion calculation also suggest that both olivine megacryst and pyroxene crystallized at a very shallow place in spite of the origin of olivine megacryst in DaG. DaG might be formed in a lava flow near the martian surface.

It is interesting that the groundmass, too, is not a liquid composition, but a cumulate. In a sense, DaG is a "double" cumulate in that it contains olivine "cumulate" xenocryst population entrained in a pyroxene cumulate groundmass. DaG cannot have behaved as a closed system. At some point a residual fractionated liquid poorer in MgO and richer in Al_2O_3 (than the groundmass composition) must have escaped as suggested by Goodrich (2003). This scenario explains why the MELTS calculation does not reproduce the observed phase assemblage and why the REE abundances of DaG are so low.

Acknowledgments

We wish to express much gratitude to Mr. O. Tachikawa for his help and technical advice during SEM analysis. We are also grateful to Mr. H. Yoshida for his help during electron microprobe analysis. We thank the Meteorite Working Group (NASA/Johnson Space Center) for supplying the thin section of EETA79001. Constructive reviews by Dr. J. Jones and an anonymous reviewer greatly improved the quality of the manuscript. This study was partly supported by Japan Society for the Promotion of Science (JSPS) Research Fellowships for Young Scientists (E.K.).

References

Borg, L.E., Nyquist, L.E., Wiesmann, H., Reese, Y. and Papike, J.J. (2000): Sr-Nd isotopic systematics of martian meteorite DaG476. Lunar and Planetary Science XXXI. Houston, Lunar Planet. Inst., Abstract #1036 (CD-ROM).

Buening, D.K. and Buseck, P.R. (1973): Fe-Mg lattice diffusion in olivine. J. Geophys. Res., **78**, 6852–6862.

Chakraborty, S. (1997): Rate and mechanism of Fe-Mg interdiffusion in olivine at 980–1300℃. J. Geophys. Res., **102**, 12317–12331.

Folco, L., Franchi, I.A., D'Orazio, M., Rocchi, S. and Schultz, L. (2000): A new martian meteorite from the Sahara: The shergottite Dar al Gani 489. Meteorit. Planet. Sci., **35**, 827–839.

Ghiorso, M. and Sack, R. (1995): Chemical mass transfer in magmatic processes. IV. A revised and internally consistent thermodynamic model for the interpolation and extrapolation of liquid-solid equilibria in magmatic systems at elevated temperatures and pressure. Contrib. Mineral. Petrol., **119**, 197–212.

Goodrich, C.A. (2002): Olivine-phyric martian basalts: A new type of shergottite. Meteorit. Planet. Sci., **37** (Suppl.), B31–B34.

Goodrich, C.A. (2003): Petrogenesis of olivine-phyric shergottites Say al Uhaymir 005 and Elephant Moraine A79001 lithology A. Geochim. Cosmochim. Acta, **67**, 3735–3772.

Herd, C.D.K., Borg, L.E., Jones, J.H. and Papike, J.J. (2002): Oxygen fugacity and geochemical variations in the martian basalts: implications for martian basalt petrogenesis and the oxidation state of the upper mantle of Mars. Geochim. Cosmochim. Acta, **66**, 2025–2036.

Jurewicz, A.J.G., Williams, R.J., Le, L., Wagstaff, J., Lofgren, G., Lanier, A., Carter, W. and Roshko, A. (1993): Technical Update: JSC system using a solid electrolytic cell in a remote location to measure oxygen fugacities in CO/CO_2 controlled-atmosphere furnaces. NASA Technical Memorandum, 104774.

McKay, G., Le, L., Wagstaff, J. and Crozaz, G. (1994): Experimental partitioning of rare earth elements and strontium: Constraints on petrogenesis and redox conditions during crystallization of Antarctic angrite Lewis Cliff 86010. Geochim. Cosmochim. Acta, **58**, 2911–2919.

McSween, H.Y., Jr. (1994): What we have learned about Mars from SNC meteorites. Meteoritics, **29**, 757–779.

McSween, H.Y., Jr. and Jarosewich, E. (1983): Petrogenesis of the Elephant Moraine A79001 meteorite:

Multiple magma pulses on the shergottite parent body. Geochim. Cosmochim. Acta, **47**, 1501–1513.
Meyer, C. (2003): Mars Meteorite Compendium - 2003. NASA Johnson Space Center, Houston, Texas, USA, (http://www/curator.jsc.nasa.gov/curator/antmet/mmc/mmc.htm).
Mikouchi, T., Miyamoto, M. and McKay, G.A. (2001): Mineralogy and petrology of the Dar al Gani 476 martian meteorite: Implications for its cooling history and relationship to other shergottites. Meteorit. Planet. Sci., **36**, 531–548.
Misener, D.J. (1974): Cation diffusion in olivine to 1400℃ and 35 kbar. Geochemical Transport and Kinetics, ed. by A.W. Hoffmann *et al*. Washington, D.C., Carnegie Inst. of Washington, 117–129.
Miyamoto, M. and Mikouchi, T. (1996): Platinum catalytic effect on oxygen fugacity of CO_2-H_2 gas mixtures measured with ZrO_2 oxygen sensor at 10^5 Pa from 1300 to 700℃. Geochim. Cosmochim. Acta, **60**, 2917–2920.
Miyamoto, M., Mikouchi, T. and Arai, T. (2002): Comparison of Fe-Mg interdiffusion coefficients in olivine. Antract. Meteorite Res., **15**, 143–151.
Wadhwa, M., Lentz, R.C.F., McSween, H.Y., Jr. and Crozaz, G. (2001): A petrologic and trace element study of Dar al Gani 476 and Dar al Gani 489: Twin meteorites with affinities to basaltic and lherzolitic shergottites. Meteorit. Planet. Sci., **36**, 195–208.
Zipfel, J., Scherer, P., Spettel, B., Dreibus, G. and Schultz, L. (2000): Petrology and chemistry of the new shergottite Dar al Gani 476. Meteorit. Planet. Sci., **35**, 95–106.